# ENERGY DISPERSION AND RELAXATION IN PROPYNAL USING

## LASER IR/VISIBLE DOUBLE RESONANCE

M.L. Lesiecki, G.R. Smith, J.A. Stewart,
and W.A. Guillory
Department of Chemistry
University of Utah
Salt Lake City, UT 84112

## ABSTRACT

The dynamics of energy dispersion in propynal has been studied over the
pressure range of 5 to 500 mtorr following excitation by a TEA $CO_2$ laser
below the dissociation threshold. Wavelength resolved spectra, using the dye
laser-induced fluorescence technique, are used to characterize the vibrational
levels that are involved in the various energy transfer process, while time-
resolved spectra are used to determine the corresponding rates. The rate
constants are extrapolated to zero pressure to obtain the regime of collision-
less intramolecular relaxation times. Mechanisms of energy dispersion
involving each of the probed vibrational levels ($v=0$, $\nu_6(v=1)$, $\nu_9(v=1)$, and
$\nu_4(v=1)$) are discussed.

## INTRODUCTION

The detailed mechanism of infrared (ir) multiphoton absorption leading
to collisionless dissociation of polyatomic molecules has received considerable
theoretical and experimental attention.[1] A vital component to understanding
the mechanism is the role played by intramolecular vibrational energy transfer
in producing a distribution of the ir pump energy among the vibrational modes
of the molecule. Experimental data concerning intramolecular vibrational
energy transfer rates in the ground electronic states of $SF_6$ and $OsO_4$ has
recently been reported.[2-5] In the case of $SF_6$, experiments were conducted

## DISCLAIMER

This report was prepared as an account of work sponsored by an agency of the United States Government. Neither the United States Government nor any agency Thereof, nor any of their employees, makes any warranty, express or implied, or assumes any legal liability or responsibility for the accuracy, completeness, or usefulness of any information, apparatus, product, or process disclosed, or represents that its use would not infringe privately owned rights. Reference herein to any specific commercial product, process, or service by trade name, trademark, manufacturer, or otherwise does not necessarily constitute or imply its endorsement, recommendation, or favoring by the United States Government or any agency thereof. The views and opinions of authors expressed herein do not necessarily state or reflect those of the United States Government or any agency thereof.

# DISCLAIMER

**Portions of this document may be illegible in electronic image products. Images are produced from the best available original document.**

using the techniques of infrared fluorescence[2] and infrared-infrared double resonance[3,4] to measure collisionless V→V energy transfer.  IR/UV double resonance was used to observe excitation of high vibrational levels of the ground electronic state and to characterize the nature of intramolecular V→V energy exchange in $OsO_4$.[5]  Double resonance techniques, in general, have been widely used to study the temporal behavior of molecules following vibrational excitation by ir lasers.[6]

In this manuscript, we report the results of studies of vibrational energy transfer and relaxation processes that occur in propynal ($C_3H_2O$) between 5 and 500 mtorr following non-dissociative excitation (0.45 $J/cm^2$) by a $CO_2$ laser at 10.49 μ (953 $cm^{-1}$).  In these experiments, we have taken advantage of both the increased sensitivity and better time resolution of pulsed dye laser probing as compared to cw ir probing techniques.  Dye laser induced fluorescence (LIF) is used to monitor the flow of energy to specific modes as well as to obtain the time profiles of the population of various vibrational levels in the ground electronic state.

## EXPERIMENTAL

The experimental apparatus has been discussed previously,[7] and only the details pertinent to these experiments are presented here.  The $CO_2$ (Gen-Tec DD250 (FWHM = 150 nsec, rep. rate = 20 Hz) laser was tuned to P(10) of the 00°1 - 10°0 transition (10.49 μ, 953 $cm^{-1}$).  This frequency corresponds to the maximum of the R-branch of $ν_6$, the C-C stretch of propynal,[8] and was chosen, in *separate* experiments, as the wavelength which when focused into the cell maximized the production of the photolysis products $C_2(a^3\Pi)$ and $CH(X^2\Pi)$.  The output beam, with a fluence of 0.45 $J/cm^2$, was collimated either to 1.0 or 2.5 cm diameter.

A Molectron UV/400/DL200 $N_2$ pumped dye laser (collimated to 0.1 or 0.2 cm diameter), directed perpendicular to the $CO_2$ laser, was used to excite vibronic transitions within the $^1A'' \leftarrow ^1A'$ electronic manifold. At a fixed time delay with respect to the $CO_2$ laser, the dye laser was scanned in wavelength while monitoring the laser induced fluorescence at 438 nm, corresponding to the $^1A'' \leftarrow ^1A'$, $4_2^0$ emission, (with a 0.25 m monochromator). The difference in the excitation spectrum with the $CO_2$ laser on and off was indicative of relative changes in the vibrational populations of the $^1A'$ ground electronic state. With the dye laser set to excite a specific vibronic transition, the delay between the two lasers could be smoothly varied and the resultant plot of LIF intensity versus delay time was analyzed to yield kinetic data. A combination of a Biomation 8100 transient recorder and a Nicolet 1070 multichannel signal averager was employed for repetitive scanning and signal averaging of both wavelength resolved and time resolved spectra. After acquisition, the data were processed on a Terak minicomputer. The time resolution (10-20 nsec) of these experiments was limited by the jitter of the $CO_2$ laser.

Propynal was synthesized,[9] purified by fractional distillations, and stored at 77°K. A freshly distilled sample was used for each experiment.

## RESULTS

Basically, two types of experiments were performed in order to determine the rates of energy dispersion of $C_3H_2O$ as a result of ir laser excitation; wavelength and time resolved spectral determinations. The wavelength resolved spectra (taken at specific delay times after firing the ir laser) indicated the response of the various vibrational levels to ir laser pumping in terms of increased or decreased population. On the other hand, time resolved spectra of specific vibrational modes characterized the various rates at which these population changes occurred. The results of both types of experiment are

presented in turn below.

## Wavelength Resolved Spectra

The excitation (wavelength resolved) spectrum of 0.300 torr of propynal recorded 10 μsec after initiation of the $CO_2$ laser is shown in Figure 1. The excitation spectrum of propynal under identical conditions, but without $CO_2$ laser excitation is also shown in Figure 1. Comparison of the two spectra allows identification of the ground electronic state vibrational modes which either increase or decrease in population as a result of ir laser absorption. The calculated vibronic transitions[10] have been labelled in Figure 1 in order to assist in the various assignments. Examination of Figure 1 clearly shows the decrease in population of the ground vibrational state ($0_0^0$ transition) and the hot bands $\nu_{12}$ and $\nu_9$. Population increases are observed in the vibronic transitions corresponding to one quanta of $\nu_6$ (primary mode pumped by the $CO_2$ laser), $\nu_4$, and possibly $\nu_{10}$. In addition, a new vibronic transition is observed near 4066 Å (marked with a ∗), shifted ~1584 $cm^{-1}$ from $0_0^0$ and probably corresponding to either of the combinations ($\nu_6 + \nu_7$), ($\nu_5 + \nu_9$), or ($\nu_{10} + \nu_8$). No other transitions were observed at 80X sensitivity to the red of $\nu_4$(v=1), as far as 3500 $cm^{-1}$ shifted from $0_0^0$.

## Time-Resolved Spectra

Time resolved spectra were obtained for the vibrationless ground state (v=0), and for v=1 of $\nu_4$ and $\nu_6$ at pressures from ~500 mtorr to ~5 mtorr (the limit set by S/N considerations). Over the msec time regime, all three levels as well as $\nu_9$(v=1) show a similar exponential return to the initial equilibrium (Fig. 2). At 100 mtorr, the decay rates are within 20% of each
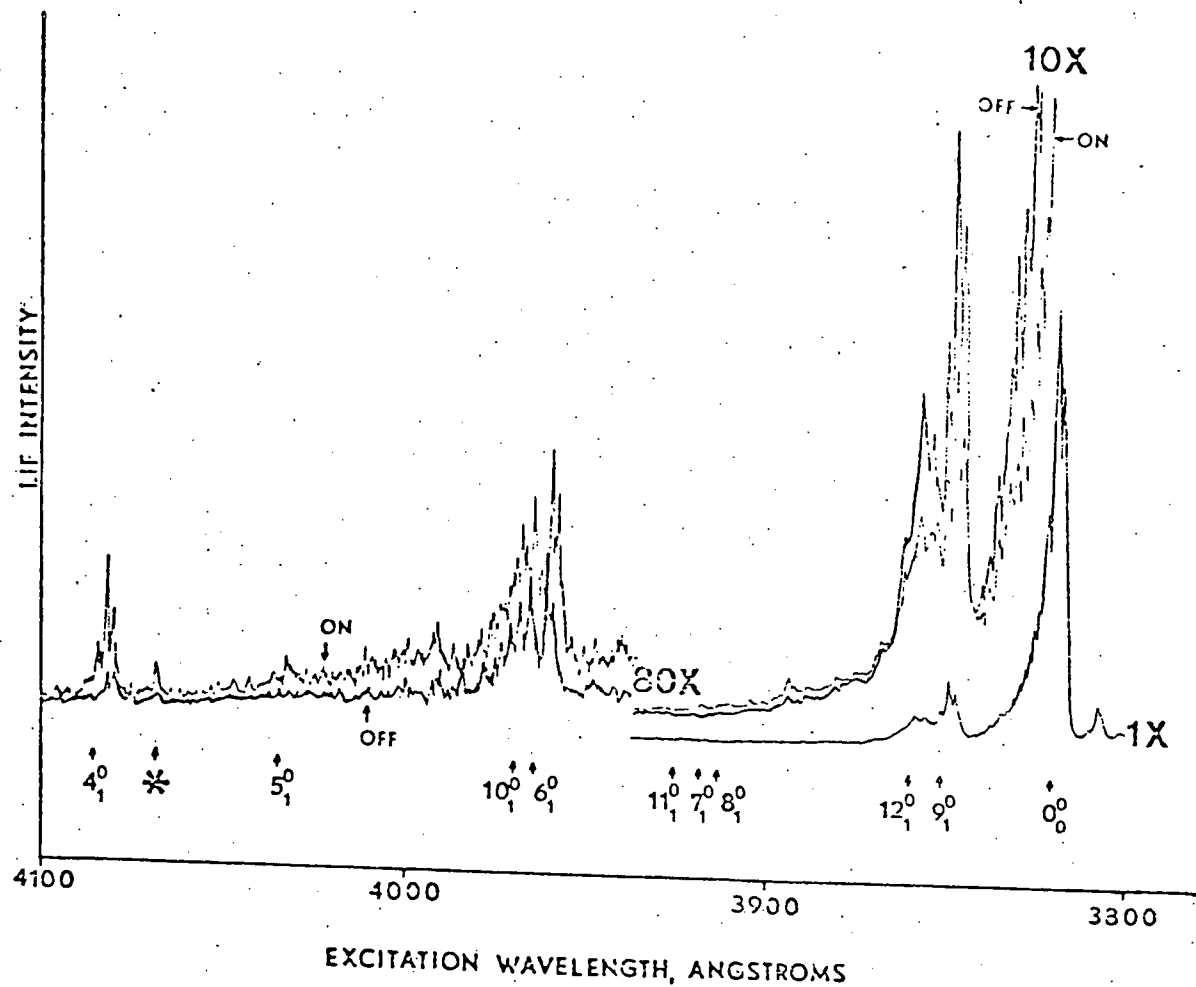
Figure 1. Excitation spectrum ($^1A'' \rightarrow {}^1A'$, $4_2^0$) of 0.300 torr propynal recorded 10 μsec after firing the $CO_2$ laser. The calculated and observed vibronic transitions involving the fundamentals $\nu_4$ through $\nu_{12}$ are labelled. The on and off designations refer to spectra recorded with or without the $CO_2$ laser excitation, respectively.
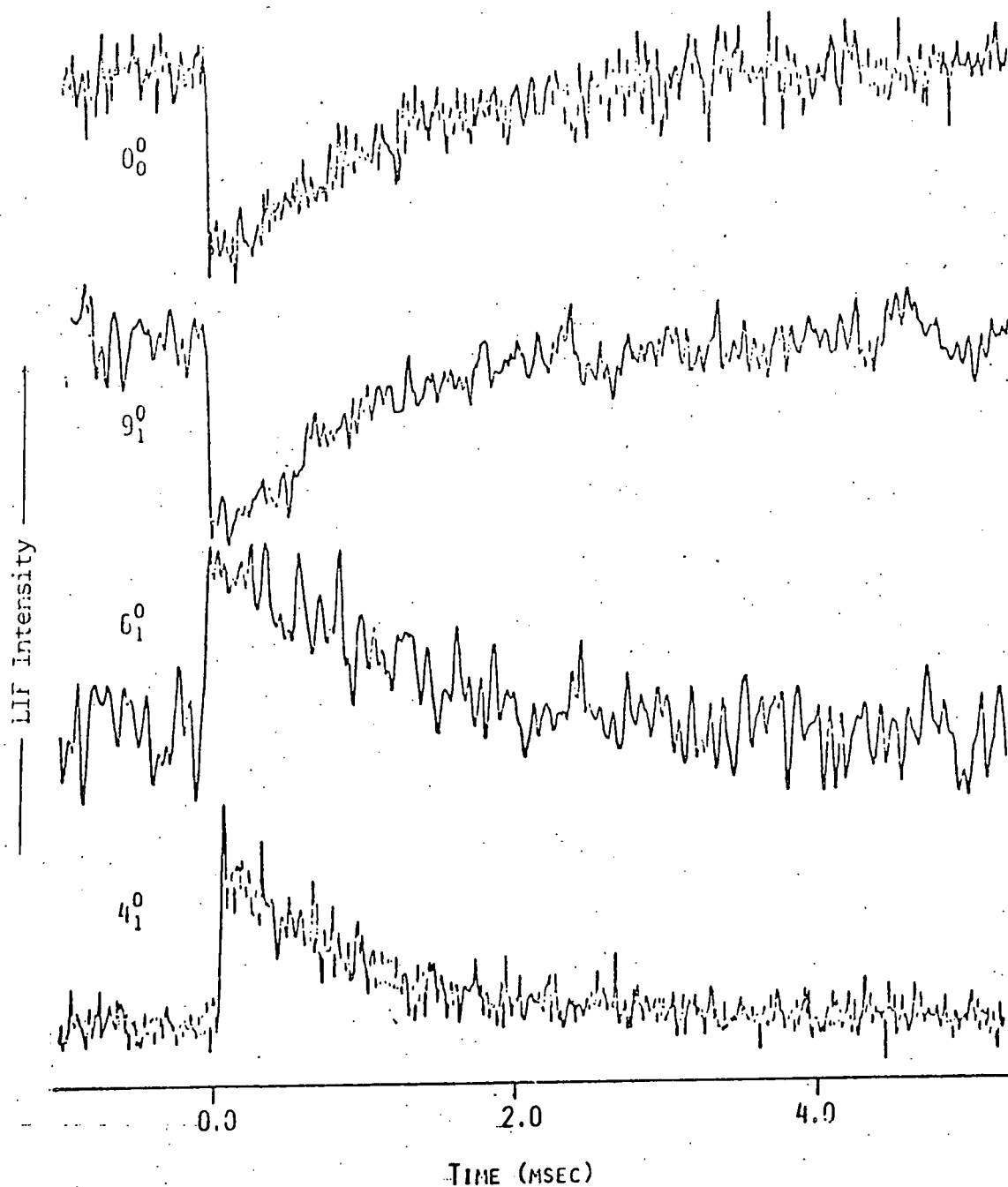
Figure 2.  Exponential rise and decay rates of $0_0^0$, $9_1^0$ and $6_1^0$, $4_1^0$ vibronic transitions, corresponding to the return of the system to the initial equilibrium after the $CO_2$ laser pulse at 0.100 torr propynal.

other and have an average value of $0.95 \times 10^3$ sec$^{-1}$, which is typical of previously observed V→R/T rate constants.[4,11] We have not investigated this temporal behavior in detail. Over the μsec time regime, the temporal behavior of the transitions corresponding to the three levels above differ significantly. Time resolved traces of $6_1^0$, $4_1^0$, and $0_0^0$ at 100 mtorr are shown in Figure 3. Although Figure 3 describes the temporal behavior of levels $v=0$, $\nu_6(v=1)$, and $\nu_4(v=1)$ at 100 mtorr, the specific shapes of the traces varied considerably with pressure and correspondingly the rate constants characterizing the various rise and decay processes.

On the basis of the observed temporal behavior (Fig. 3) of each vibrational level, we assumed a kinetic scheme, derived the corresponding integrated equation characterizing the observed vibrational level, and adjusted the various rate constants to fit the experimental curves as a function of pressure. These data were fit to the observed curves by the use of published $\chi^2$ minimization algorithms.[12] In order to avoid over-determining the fits, the simplest kinetic schemes possible were used, therefore specific physical processes should not necessarily be ascribed to the resulting parameters. The kinetic schemes used were dictated by the shapes of the curves as a function of pressure. The level $v=0$ simply decreased to a different equilibrium population over the μsec time regime. Thus, this level was modelled by the simple reversible process

$$A \underset{k_2}{\overset{k_1}{\rightleftharpoons}} B \qquad (1)$$

where A corresponds to the set of rotational levels probed by the $0_0^0$ vibronic transition and B is any level (or levels) which participate in the reversible reaction. The concentration of B is assumed to initially be zero. The actual form of the equation fit to the data is
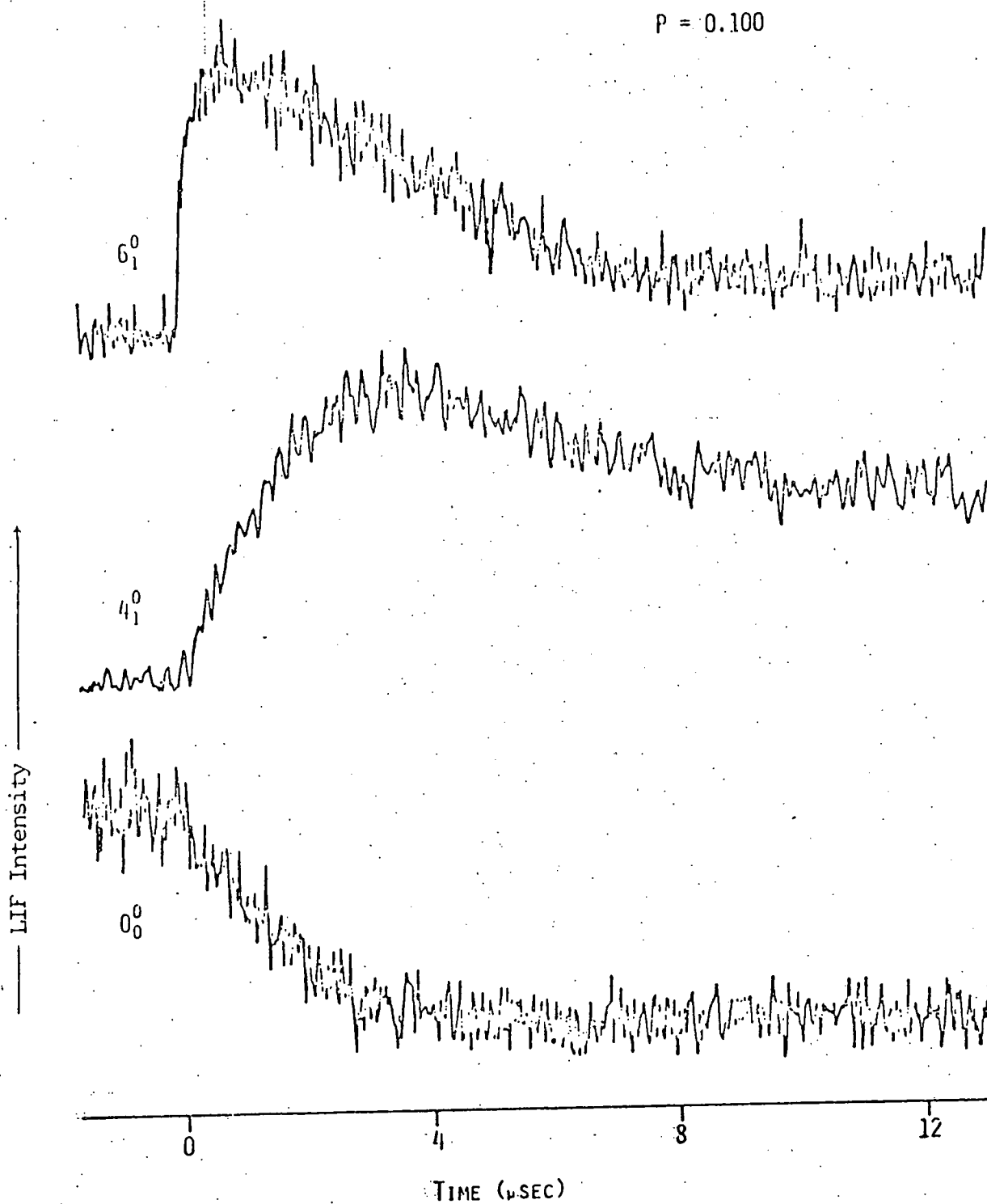
$$P = 0.100$$



Figure 3. Time-resolved spectra of the $6_1^0$, $4_1^0$, and $0_0^0$ vibronic transitions ($^1A'' \leftarrow {}^1A'$) of 0.100 torr of propynal.

$$A(t) = \frac{k_1 A_0}{k_1 + k_2} \exp - [(k_1 + k_2) t] + \frac{k_2 A_0}{k_1 + k_2} \qquad (2)$$

where $k_1$ and $k_2$ were adjusted to fit the pressure varying curves.

For the $\nu_6(v=1)$ and $\nu_4(v=1)$ levels, a more complicated expression was needed to fit the data. Both of these levels rise to a maximum and then decrease to equilibrium populations different from those initially. An equation which suitably describes this behavior is obtained by integrating the differential equation for B, using the kinetic scheme

$$A \xrightarrow{k_1} B \underset{k_3}{\overset{k_2}{\rightleftharpoons}} C \quad . \qquad (3)$$

We obtain

$$B(t) = \frac{A_0(k_1 - k_3)}{(k_2 + k_3 - k_1)} \exp(-k_1 t) - \frac{A_0 k_1 k_2}{(k_2 + k_3 - k_1)(k_2 + k_3)} \exp[-(k_2 + k_3)t]$$

$$+ \frac{A_0 k_3}{(k_2 + k_3)} \qquad (4)$$

In this case, we monitor B, which corresponds to either level $\nu_6(v=1)$ or $\nu_4(v=1)$. There are, strictly speaking, four adjustable parameters in the above equation, the three rate constants and $A_0$. The latter however, is simply used as a scale factor.

It should be noted that quoted error limits represent the reproducibility of the experiment only. Limits are given for the constants derived at a certain pressure when there are several measurements at that pressure. They are quoted at the 80% confidence level. On the other hand, least squares parameters have error limits based on the standard deviation of the fit, and are quoted at the 90% confidence level.

## Ground Vibrational Level (v=0)

To treat the data for the decrease in intensity observed while monitoring the $0^0_0$ (bandhead) transitions, we have assumed that the levels being monitored (A) equilibrate with the rotational levels (B) depleted as a result of the $CO_2$ laser pumping. It should be pointed out that we are referring to the apparent *quasi-equilibrium* between the vibrational modes illustrated in Figure 3 after 8 μsec and extending to ~1 msec. Using the computer fitting procedures described above, the *net* rate constant characterizing the approach to equilibrium is, $k_1 + k_2 = (1.10 \pm 0.16) \times 10^6 P$ sec$^{-1}$ torr$^{-1}$ + $(4.23 \pm 0.17) \times 10^5$ sec$^{-1}$. The expressions which characterize the variation of $k_1$ and $k_2$ versus pressure below ~0.200 torr are $k_1 = (6.13 \pm 0.39) \times 10^5 P$ sec$^{-1}$ torr$^{-1}$ + $(4.54 \pm 0.38) \times 10^4$ sec$^{-1}$ and $k_2 = (5.46 \pm 1.49) \times 10^5 P$ sec$^{-1}$ torr$^{-1}$ + $(3.70 \pm 0.16) \times 10^5$ sec$^{-1}$. All rate constants were obtained from least squares fits at 90% confidence.

## $\nu_6$(v=1) Level

In the modelled scheme for $\nu_6$(v=1) described by Eq. (3), $k_1$, $k_2$, and $k_3$ are composite rate constants characterizing several elementary processes; $k_1$, $k_2$, and $k_3$ characterize respectively, all processes (radiative and non-radiative) that *initially* populate the observed level $\nu_6$(v=1), all processes that deplete $\nu_6$(v=1), and all processes that populate $\nu_6$(v=1) in establishing and maintaining the quasi-equilibrium to ~1 msec. The risetime of the $6^0_1$ transition was extremely fast, particularly at pressures above 0.200 torr. A plot of these constants versus pressure below 0.100 torr yields a straight line characterized by $k_1 = (2.12 \pm 0.08) \times 10^7 P$ sec$^{-1}$ torr$^{-1}$ + $(1.20 \pm 0.38) \times 10^5$ sec$^{-1}$. This expression (exclusive of the intercept) gives rise to a cross section of $\sigma = 129$ Å$^2$. Assuming the extrapolated intercept (P≈0) to be the

radiative contribution, it makes an additional ~20% contribution to $\sigma(166 \text{ Å}^2)$ at 0.020 torr.

The rate constants $(k_2+k_3)$ characterizing the approach to equilibrium was considerably slower than $k_1$ at pressures above 0.100 torr, but comparable at lower pressures. A plot of $(k_2+k_3)$ versus pressure was linear over the range 0.100 - 0.500 torr with $(k_2+k_3) = (8.18 \pm 0.44) \times 10^5 P \text{ sec}^{-1} \text{ torr}^{-1} + (2.52 \pm 0.15 \times 10^5 \text{ sec}^{-1}$. Below 0.100 torr, the rate constant appeared to level off at ~3.5 $\times 10^5 \text{ sec}^{-1}$. The fitted constants for $k_2$ were linear as a function of pressure to ~0.100 torr and characterized by $k_2 = (5.12 \pm 0.61) \times 10^5 P \text{ sec}^{-1} \text{ torr}^{-1} + (2.55 \pm 0.21) \times 10^5 \text{ sec}^{-1}$, and below ~0.100 torr it also appeared to level off at ~3.0 $\times 10^5 \text{ sec}^{-1}$. The values of $k_3$ were a linear function of pressure over the entire pressure range and appeared to extrapolate to zero as $P \rightarrow 0$; $k_3 = (3.00 \pm 0.22) \times 10^5 P \text{ sec}^{-1} \text{ torr}^{-1}$.

### $\nu_4(v=1)$ Level

The modelled scheme for $\nu_4(v=1)$ is the same as that used for $\nu_6(v=1)$, where again $k_1$, $k_2$, and $k_3$ are composite constants. Each of these constants have the same meaning as described in the $\nu_6(v=1)$ section above, except that $k_1$ does not have a radiative component in this case. The $k_1$ component was approximately linear over the entire pressure range (0.358 to 0.0101 torr) and characterized by the expression $k_1 = (2.75 \pm 0.04) \times 10^6 P \text{ sec}^{-1} \text{ torr}^{-1} + (1.00 \pm 0.05) \times 10^5 \text{ sec}^{-1}$. It is interesting to note that the slope of $k_1$ is smaller than the gas kinetic slope by a factor of 3, which corresponds to an energy deficit $[\exp-(1.44 \ \Delta\epsilon/T)]$ of ~200 $\text{cm}^{-1}$.

The variation of $k_2$ with pressure was very surprising, having a shape very similar to a normal unimolecular constant versus pressure plot. The expression which characterizes the fall off pressure of the rate constant

$k_2$ is $[P_B] = k_\infty/k_a$; where $P_B$ is the pressure of [B] at $k_\infty/2$ ($\sim 2.0 \times 10^5$ sec$^{-1}$), $k_\infty$ is the limiting value of $k_2$ ($\sim 4.0 \times 10^5$ sec$^{-1}$), and $k_a$ is the rate constant for activation of B. Assuming $k_a[\pi\sigma^2 v \exp-(\epsilon^*/kT)]$ to be exactly gas kinetic (as a lower limit, $\epsilon^* = 0$), the calculated value of $P_B = 0.023$ torr. This is the predicted pressure of $B(\nu_4, v=1)$, whereas our plot involved the initial pressure of propynal.

The variation of $k_3$ with pressure appeared to be bimodal; that is, having two linear components as a function of pressure. The low pressure component (0.200 - 0.010 torr has $k_3$ 1.0 $\times 10^6 P$ sec$^{-1}$ torr$^{-1}$ with an intercept of essentially zero.

## DISCUSSION

The objective of this manuscript is to characterize the overall nature of vibrational energy dispersion and rotational relaxation that occur in a moderate size polyatomic molecule ($HC\equiv C-C{\overset{\nwarrow O}{\underset{\searrow H}{}}}$). These energy flow processes are studied in the absence of laser-induced fragmentation when propynal is excited below its vibrational quasi-continuum with an unfocused $CO_2$ laser.

In Figure 3, all three vibronic transitions level off at intensities different from those initially by 8 μsec after initiation of the $CO_2$ laser pulse. The spectrum shown in Figure 1 represents a vertical cut of Figure 3, taken at 10 μsec. In practice, a wavelength resolved spectrum of the levels of interest can be constructed at any delay time of interest from Figure 3. Since the time-resolved spectrum of Figure 2 is indicative of V→R/T processes,[4,11] it appears that the level portions of Fig. 3 represent *quasi-equilibration* among the vibrational modes at a higher temperature, while remaining rotationally and translationally at room temperature. Thus, we assume that the modelled constants essentially correspond to processes that disturb the initial equilibrium and characterize the return to

quasi-equilibrium, principally among the vibrational modes.

In order to probe the temporal population change of the ground vibronic level, the dye laser was tuned to the peak of the $\hat{0}_0^0$ transition corresponding to the bandhead near 3820 Å. The intensity of this particular transition is due to the heading of the various $Q_K$ branches of low K, and J values typically between 50 and 80.[13] Since the probe frequency is at least 260 $cm^{-1}$ above the J = 30 rotational level, which is pumped by the $CO_2$ laser, we are monitoring rotational relaxation into the hole burned by the $CO_2$ laser. Assuming a constant rotational temperature, the ratio of the laser induced fluorescence intensity after establishing quasi-equilibrium ($I_e$) to that before the $CO_2$ laser initiation ($I_i$), $I_e/I_i$, represents the fraction of molecules depleted or pumped from the ground vibrational level. This fraction varies from ~60% at 0.50 torr where collisional refilling is efficient to an extrapolated 5% as P→0. This fraction compares with the calculated percentage in J = 30, depleted by the $CO_2$ laser without refilling, of 4.7%.

The time evolution of $\nu_6$(v=1) was the fastest process observed in these studies, having a slope approximately twice that of gas kinetic. This observation clearly indicates that the near resonant energy transfer processes (within the mainfold of the pumped mode) dominate those occurring in this system. Since the rate constant (which is approximately a factor of 2 greater than gas kinetic) has both radiative and collisional components, we reason that the factor of 2 might arise from the following processes,

$$\nu_6(v=0) + 2h\nu(ir) \rightarrow \nu_6(v=2) \qquad (5)$$
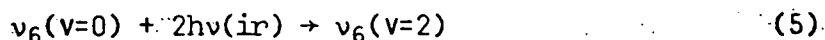
involving the direct absorption of two photons, probably in multiple or sequential fashion, followed by

$$\nu_6(v=2) + \nu_6(v=0) \rightarrow 2\nu_6(v=1) \quad . \qquad (6)$$
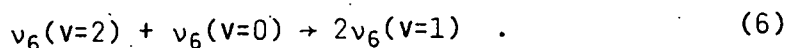
In fact, we estimate the number of photons absorbed per molecule to be 3-4 and 4-5 respectively, at 0.500 and 0.200 torr from transmitted energy measurements. Although we were unable to directly observe levels $\nu_6(v=2, 3, \text{etc.})$, they are, in addition to radiative pumping, also probably generated in collisional fashion via

$$\nu_6(v=n) + \nu_6(v=1) \rightarrow \nu_6(v=n+1) + \nu_6(v=0), \quad n>0 \qquad (7)$$
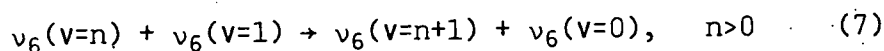
Very fast near resonant V→V energy transfer has been observed in other systems[14] and are known to account for *up-the-ladder* transfer from v=1 to v=2 of the same normal mode in a polyatomic molecule.

The loss of $\nu_6(v=1)$ via B $\xrightarrow{k_2}$ C has a $k_2$ versus pressure slope ($5.11 \times 10^5$ sec$^{-1}$ torr$^{-1}$) which is approximately equal to the slope of $k_2$ for v=0 ($5.46 \times 10^5$ sec$^{-1}$ torr$^{-1}$). Thus, the loss of population from $\nu_6(v=1)$ might be a major contributor to establishing the quasi-equilibrium of the v=0 level by collisional intermolecular energy transfer. It ($k_2$ for $\nu_6$, v=1) extrapolates to a P→0 intercept of $2.55 \times 10^5$ sec$^{-1}$, which probably corresponds to the rate constant characterizing intramolecular energy transfer to a nearby vibrational level(s) i.e. $\nu_{10}(981.2$ cm$^{-1})$. The value of $k_3$, which characterizes the establishment of the quasi-equilibrium, appears to be principally indicative of intermolecular energy transfer processes, since it falls off very rapidly with decreasing pressure and has an extrapolated intercept of zero.

The relatively rapid rise of $\nu_4(v=1)$ is predicated on inter and intramolecular energy transfer, principally from $\nu_6(v=2)$, which is presumably populated either by fast collisional pumping (Eq. 7) and by optical pumping (Eq. 5).

$$\nu_6(v=2) + \nu_4(v=0) \rightarrow \nu_6(v=0) + \nu_4(v=1) + 180 \text{ cm}^{-1} \qquad (8)$$
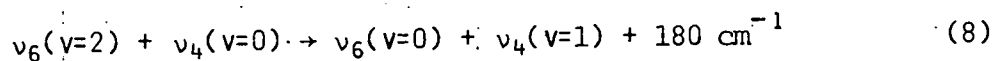
where $\nu_6$ and $\nu_4$ may be vibrational modes of two different molecules or of a single molecule. The former process is intermolecular V→V energy transfer whereas the latter is a sum of collision-assisted and collisionless V→V energy transfer. The dominance of each of these processes depends upon the total system pressure in pure propynal. Support for Eq. (8) is provided by the fact that the slope of the risetime constants, $k_1$, versus pressure is roughly equal to the slope of the gas kinetic collision constant having an energy deficity of ~200 cm$^{-1}$. Extrapolation to P→0 resulted in an intercept of $1.0 \times 10^5$ sec$^{-1}$, or a relaxation time of 10 μsec as the truly collisionless intramolecular energy transfer regime is approached.

As we pointed out in the Results, the modelled behavior of $k_2$ for $\nu_4(v=1)$ versus pressure was strikingly similar to a typical unimolecular rate constant in the fall off region. Interpreting the data in this manner, we calculated $P_B \simeq 0.023$ torr at $k_\infty/2$, assuming that $k_a$ effectively activates a molecule to reaction on every collision. Although we have no actual measurements of $P_B$, the calculated pressure was 50% smaller than $P_{propynal}$ (0.045 torr). It is interesting to note that the failure of this prediction (using the assumption of $k_a$ above) usually results in a much higher pressure normally in the $k_\infty$ region, whereas this result not only predicts it to be in the fall off region but corresponding to 50% conversion of ground state propynal to $\nu_4(v=1)$. The nature of $k_3$ appears to be similar to $k_3$ for $\nu_6(v=1)$, in that the establishment of quasi-equilibrium is principally intermolecular relaxation (P→0 intercept of zero).

It is obvious that this study is an initial attempt to determine the rates and characterize the mechanisms of relaxation processes which are vital to

understanding not only infrared multiphoton absorption but the dynamics of energy transfer in general. The unique aspect of this study is the application to a polyatomic molecule where some detail is possible and the extension of these determinations to the collisionless pressure regime. Current experiments are now in progress to study these energy transfer processes at higher levels of excitation, and with shorter $CO_2$ laser pulses, and lower pressures.

## ACKNOWLEDGEMENTS

## REFERENCES

1.  a.  R.V. Ambartzumyan and V.S. Letokhov, in Chemical and Biochemical Applications of Lasers, Vol. III (B.C. Moore Ed.), pp. 167-316, Academic Press, New York (1977);
    b.  C.D. Cantrell, S.M. Freund, and J.L. Lyman, "Laser Induced Chemical Reactions and Isotope Separation", to appear in Laser Handbook, Vol. III, North-Holland Publishing Co., Amsterdam (1978).

2.  D.S. Frankel, Jr. and T.J. Manuccia, Chem. Phys. Lett., 54, 451 (1978).

3.  D.S. Frankel, Jr., J. Chem. Phys., 65, 1696 (1976).

4.  T.F. Deutsch and R.S.J. Brueck, J. Chem. Phys., 70, 2063 (1979).

5.  R.V. Ambartzumyan, Yu. A. Gorokhov, V.S. Letokhov and G.N. Makarov, JETP Lett., 22, 43 (1975).

6.  Laser and Coherence Spectroscopy (J.I. Steinfeld ed.), Chap. 1, Plenum, New York (1978).

7.  M.L. Lesiecki and W.A. Guillory, J. Chem. Phys., 69, 4572 (1978).

8.  J.C.D. Brand, and K.J.G. Watson, Trans. Farad. Soc., 56, 1582 (1960).

9.  J.C. Sauer, Org. Syn. Collect., <u>4</u>, 813 (1963).

10. C.A. Thayer, A.V. Pocius, and J.T. Yardley, J. Chem. Phys., <u>62</u>, 3712
    (1975) contains an extensive list of references on the spectroscopy of
    propynal.

11. R.C.L. Yuan and G.W. Flynn, J. Chem. Phys., <u>57</u>, 1316 (1972).

12. P.R. Bevington, <u>Data Reduction and Error Analysis for the Physical Sciences</u>,
    McGraw Hill, New York (1969).

13. J.C.D. Brand, J.H. Callomon, and J.K.G. Watson, Disc. Farad. Soc., <u>35</u>,
    175 (1962).

14. B.L. Earl, P.C. Isolani, and A.M. Ronn, Chem. Phys. Lett., <u>39</u>, 95 (1976).